IEEE Access
Multidisciplinary ⋮ Rapid Review ⋮ Open Access Journal

Received January 13, 2021, accepted January 19, 2021, date of publication January 27, 2021, date of current version November 30, 2021.

Digital Object Identifier 10.1109/ACCESS.2021.3054929

Spectral Design of Light-Emitting Diodes for Plant Photosynthesis Based on Quantum Dots

ZILEI LIU[1], FENG LI[1], GAOXIANG HUANG[1], JIAHU WEI[1], GUANGYU JIANG[1], YAN HUANG[1], XIAO JIN[2], AND QINGHUA LI[2]

[1]Jiangxi Engineering Laboratory for Optoelectronics Testing Technology, Nanchang Hangkong University, Nanchang 330063, China
[2]Guangdong Provincial Key Laboratory of Development and Education for Special Needs Children, Lingnan Normal University, Zhanjiang 524048, China

Corresponding author: Feng Li (lifengnchu@163.com)

This work was supported in part by the Natural Science Foundation of China under Grant 11774141, Grant 62005113, and Grant 11864026; in part by the Natural Science Foundation of Jiangxi Province under Grant 20202ACBL202004, Grant 20192BBF60001, Grant 20192ACBL21045, and Grant 20181BBE50022; in part by the Key Scientific Research Foundation in Higher Education of Guangdong, China, under Grant 2020ZDZX3034; in part by the Science and Technology Project of the education department of Jiangxi Province, China, under Grant GJJ180536; and in part by the Graduate Student Innovation Fund of Nanchang Hangkong University under Grant YC2019058.

ABSTRACT Light is one of the five indispensable factors for plant growth. Green houses and plant factories have advantages of growing vegetables off-season and high production. However, artificial lighting occupies most of the running cost during the operation of plant factories, and intelligent and programmable light-emitting diodes (LEDs) have been considered to be used as growing lamps to save energy. Taking both the photosynthetic and the visual performances into consideration, luminescent spectrum of LEDs based on quantum dot (QD) materials is designed and optimized according to the photosynthetic action spectrum (PAS) of plants. In our calculation, the three-band QD-based LEDs (QLEDs) show a highest photosynthetic action factor (PAF) of 8.088 and a highest induced photosynthetic index (IPI) of 4.012. The four-band QLEDs show a highest PAF of 7.689 and a highest IPI of 3.818. CdZnS/ZnS and CdZnS/ZnSe QDs are also synthesized for fabricating three- and four-band QLEDs. Investigations of the photosynthetic and the vison performances on these devices are consistent with those theoretical simulation results. Both the simulation and the experimental results show that either the three- or the four-band QLEDs has better photosynthetic parameters than those of the conventional light sources. The fabricated four-band QLED under different applied current exhibits a highest PAF of 2.6942 and a highest IPI of 1.3621. For the vison performances, the four-band device demonstrate a highest CRI of 93 and a highest CCT of 2053 K. Despite the visual performances of the four-band QLEDs show improvement than those of the three-band ones, they still need to be improved to offer better visual experience for human eyes. With further investigation on the synthesis of emission tunable QD materials and the optimization of the spectrum, highly efficient QLEDs with both good photosynthetic and visual performances are expected to be applied in the field of growing lamps.

INDEX TERMS Induced photosynthesis index, light-emitting diodes, photosynthetic action factor, quantum dots.

I. INTRODUCTION

Plant cultivation with artificial lighting is of great significance in long-term space-mission, growing pollution-free organic vegetables, dealing with the diminishing land resources and so on [1], [2]. Plant factory has developed over sixty years since it was setup in Denmark [3] . Up to now, many kinds of leaf and root vegetables including lettuces, cabbages, potatoes and tomatoes have been planted successfully in indoor plant factories [4]–[7]. Light, temperature, humidity, air and nutrition are the five indispensable factors for plant growth. Indoor plant factory, which is not affected by seasons, weather and other outside environment factors, has higher production efficiency than that of a sunlight/artificial light combined system. However, for indoor plant factories in which only artificial light such as high-pressure sodium lamps or fluorescents are used for the photosynthesis of plants, electricity for lighting accounts for about 40% of the total running cost for the vegetable production. Besides, heat release during the illumination of

The associate editor coordinating the review of this manuscript and approving it for publication was Jiajie Fan.

high-pressure sodium lamps or fluorescents will lead to the temperature variation of environment. Therefore, there is extra electricity cost for the air conditioning. To balance the production and the energy consumption in indoor plant factories, reducing the running cost especially the electricity consumption has received extensively attention and enormous hard work [8], [9].

Light-emitting diodes (LEDs) have the advantages of high energy efficiency, low radiant heat, increasing number of emission wavelengths and so on. Furthermore, their spectral composition and light intensity can be controlled easily. By integrating them with different sensors and controllers, smart lighting systems can be built to meet different needs. As the price declines, LEDs, as supplementary lighting sources or full-time ones, have found many opportunities to incorporate the plant growth in greenhouses or plant factories [10]. Studies on photobiology and photomorphogenic show that the spectral power distribution (SPD) of a light source have important effects on the plant physiological activities, which means light of different wavelengths have different effects on the growth stages of different plant species, owing to their different combination of photopigments for photosynthesis [11]–[14]. Therefore, spectral composition and light intensity should be adjusted timely in different stages for different plants to ensure the satisfied production [11], [15]. The higher the matching degree between the SPD of the light source and the photosynthesis action spectrum (PAS, $P(\lambda)$) of a certain growth stage (germination, leaf, stem, etc.) of a certain plant species, the higher the photosynthesis efficiency is. There are three basic classes of pigments: chlorophylls (chlorophyll a, chlorophyll b, etc.), carotenoids (carotene, fucoxanthin, etc.) and phycobilins (phycoerythrin, phycocyanin) [16]. These pigments have different absorption peaks and each absorbs only a narrow range of wavelengths, leading to the different shapes of their PAS curves [16], [17]. To capture more light energy for photosynthesis, there are several pigments in a plant vegetable [18], [19]. Therefore, the final PAS of a stage of a plant is relative to the concentration of each pigments and their respective PAS curves [20].

It seems that the diversity of pigments and the concentration variations during growth make it difficult to obtain a light source that, once and for all, matches the PAS spectrum. Fortunately, three considerations that complement each other can settle this problem. Firstly, monochrome LED chips of various colors (including red, yellow, green, blue, etc.) have been mass-produced and commercialization. It is completely feasible to use the combination of these monochrome LED chips according to the absorption peaks of the pigments. Secondly, these chips can be driven by independent currents respectively, so that the luminous intensity of each chip can be adjusted, so as to the spectra shape of light source [14], [21]. Finally, chlorophyll a (CL a) and chlorophyll b (CL b) are the most common but important pigments for photosynthesis in most of the vegetables and green plants, whose absorption peaks are mainly distributed in the red and blue bands, or, specifically, at $\sim$ 450 nm and $\sim$ 660 nm, respectively [17]. However, the concentration of other pigments such as carotene may be less than that of CL a or CL b, they have strong absorption to light of some other bands. Therefore, the PAS of plants can be regarded as a combination of these pigments [17], [22]. Based on early many detailed research results, a standardized PAS that fits an averaged vegetation type has been adopted and number as DIN 5031-10 by the German Institute for Standardization.) [23]. The standardized PAS enables the designing and manufacturing of conventional growing lamps for most of the green plants.

However, LEDs based on semiconductor P-N junctions usually emit narrow-band light. Moreover, spectra with only narrow-band blue and red compositions often show low color rendering index (CRI) leading to unappealing visual perception of human eyes. By integrating rare-earth phosphors with blue InGaN LEDs, higher CRI so that better visual perception can be obtained [24]. However, the availability of peak wavelengths and full-width of half-maximums (FWHMs) of rare-earth phosphors is limited, and the flexibility of spectral design for photosynthesis is restricted.

Semiconductor quantum dots (QDs) are a kind of newly optoelectronic materials, and they have many unique properties including solution processability, low cost and wide color gamut. Their emission properties can also be adjusted tactfully by varying the element composition, dot size, particle structure or the combination of these [25], [26]. Therefore, QDs have been applied in many fields such as LEDs, solar cells, bioimaging, etc. [27]. Electroluminescent red, green and blue LEDs based on QDs have been assembled successfully. By using the combination of QDs of different emission colors as phosphors, photoluminescent LEDs also demonstrate attractive properties such as high color rendering index (CRI), high scotopic/photopic ratio, high LER, etc. [28]–[30]. Up to now, the emission wavelengths of QDs have covered the whole range of visible light and provide the spectral design for plant photosynthesis according to the PAS curve with more choices and flexibility.

II-VI QDs, including CdS and CdSe, have benn explored extensively. Though the introduction of Zn, the emission wavelength of obtained CdZnS or ZnCdS QDs can be adjusted by controlling the Cd/Zn ratio [31]. Moreover, inorganic shell or shells passivating the surface defects is helpful for the improvement photoluminescence (PL) quantum yields and widening the wavelength emission range [32]–[34]. Here in this study, on the one hand, we perform design and optimization the spectra of QD-based LEDs (QLEDs) according to the PAS curve which adopted by the German Institute for Standardization. Double Gaussian model [35] is used to described the emission spectra of QDs and QLEDs, and photosynthetic action factor (PAF) and induced photosynthesis index (IPI) are used to evaluate the influence of the QLEDs of different SPDs on the photosynthesis of plants. However, an indoor plant factory is also a workplace for staff. On the condition that ensuring expected production, the staff's personal environmental experience and physical health should also be taken into consideration, because research results

have suggested that wrong indoor light during day and light will disturb the temper and the regular circadian rhythms and lead to some diseases risks [36]. Hence, visual perception, which is very important for the human visual experience, should be also taken into consideration when optimizing the spectra. On the other hand, ZnCdS/ZnS and ZnCdS/ZnSe QDs with different emission wavelength are also synthesized for the fabrication of QLEDs. Both the photosynthetic and the vision performances of the fabricated QLEDs are investigated, and the experimental results are consistent with the simulation ones. Owing to the flexible adjustment of the emission wavelength, the spectra shape, so as to the expected photosynthetic and vison performance of the QLED can be easily realized.

II. THEORY

A. PHOTOSYNTHETIC ACTION FACTOR (PAF) AND INDUCED PHOTOSYNTHESIS INDEX (IPI)

Studies have shown that light with higher red refractions can effectively promote the growth of plant height, leaf number, leaf width, and leaf area, while higher blue refractions favor photosynthetic performance and the accumulation of carbohydrates [18]. However, light emitted by a simple white artificial lighting system may not be effectively utilized by plant photosynthesis because its spectral distribution does not conform to the spectral range that plant photoreceptors can perceive, and even affect the photosynthesis of plants when certain bands of light are missing. Photosynthetically active radiation (PAR) are the wavelengths of light within the visible range of 400 to 700 nm that are critical for photosynthesis. In order to evaluate how efficient a light source is at creating PAR, photosynthetic photon flux (PPF) has been proposed. Assuming all photons between 400 and 700 nm have equal weight to drive photosynthesis, PPF means the total amount of photos produced by a lighting system each second [37]–[39]. In fact, a blue photon has more energy than a red one. Moreover, specific wavelengths are absorbed differently by various pigments. Therefore, a yield photon flux was proposed to measure PAR more accurately [38]. Besides, similar to the photon quantities including luminous efficacy of radiation (LER) derived from radiation ones based on the spectral sensitivity function of human eyes, photosynthetic quantities including photosynthetic luminous efficacy of radiation (PLER) derived from radiation ones have been proposed to evaluate the effect of artificial light sources on the photosynthesis of green plants [17], [22]. PAF is also defined as the ratio of PLER to LER and written as followed.

$$\mathrm{PAF} = PLER/LER \tag{1}$$

In detail, PLER and LER are written as:

$$\begin{aligned} PLER &= K_{p0}\int_{380\ nm}^{780\ nm} P(\lambda)S(\lambda)d\lambda \Big/ \int_{0}^{\infty} S(\lambda)d\lambda \\ LER &= K_{0}\int_{380\ nm}^{780\ nm} V(\lambda)S(\lambda)d\lambda \Big/ \int_{0}^{\infty} S(\lambda)d\lambda \end{aligned} \tag{2}$$

in which K_{p0} is 683 plm/W meaning the maximal spectral photosynthesis value, K_0 is 638 lm/W meaning the maximal spectral luminous efficacy for photopic vision, and $S(\lambda)$ is the SPD of the light source. LER is an important measure to evaluate the efficiency of a white light source for lighting, and it denotes the fraction of radiant power perceived by human eyes to observe objects. That's why the spectral sensitivity function of human eyes must be taken into consideration. Correspondingly, with a same logical thinking, $P(\lambda)$ should also be considered to evaluate how efficient a light source is at driving photosynthesis. It can be seen from Equation (2) that *PLER* indicates the fraction of radiant power used for driving photosynthesis. For a white light source, a higher LER is desired since it suggests more optical energy is radiated at the wavelengths where the eye is sensitive, that is to say, less power loss. Similarly, a growing lamp with a higher *PLER* is desirable, as it means less energy is radiated at the wavelengths where the pigments do not absorb. Therefore, *PAF* means the percentage of the luminous flux driving photosynthesis accounting for that human eyes receive.

Besides, by taking PAS into consideration, induced photosynthesis index (IPI) was also proposed to evaluate the photosynthetic performance of a light source. IPI is defined as:

$$\mathrm{IPI} = \frac{\int_{380\ nm}^{730nm} \phi_{n(\mathrm{lamp})}(r,\lambda)P(\lambda)d\lambda}{\int_{380\ nm}^{730\ nm} \phi_{n(D65)}(r,\lambda)P(\lambda)d\lambda} \tag{3}$$

where ϕ_{n} is the normalized SPD of a light source, and the normalization method is given by Equation (4) below, in which $\phi(\lambda)$ is the unnormalized SPD of the light source and $V(\lambda)$ is the photopic spectral sensitivity function of human eyes. D65 is a CIE standard illuminant, whose spectrum corresponds roughly to a midday sun in Western/Northern Europe[40].

$$\phi_{\mathrm{n}}(\lambda) = \frac{\phi(\lambda)}{\int_{380\ nm}^{730\ nm} \phi(\lambda)V(\lambda)d\lambda} \tag{4}$$

It will be more reasonable to use PAF and IPI to evaluate the photosynthetic performance of a light source, because both of them take into account the PAS curve of plants. In any case, the effect of LED light source on photosynthesis is closely related to the matching degree between its SPD and the PAS curve. Here, the PAS which is used by the German Institute for Standardization and numbered as DIN 5031-10 is selected to simulation the photosynthetic performance QLEDs [22]. This PAS curve was obtained mainly according to the response of Cl a and Cl b, the most common pigments in photosynthesis of green plants, in line with the photosynthesis of most green plants. By using the original data from references [22], the photopic sensitivity action curve $V(\lambda)$ of human eyes and the PAS curve $P(\lambda)$ of plants are given in Fig. 1a, and the SPD of D65 is given in Fig. 1b.

B. DESCRIPTION OF SPECTRUM MODEL

Many models, including Gaussian model, double Gaussian model, Yoshihiro's model and He's model, have been

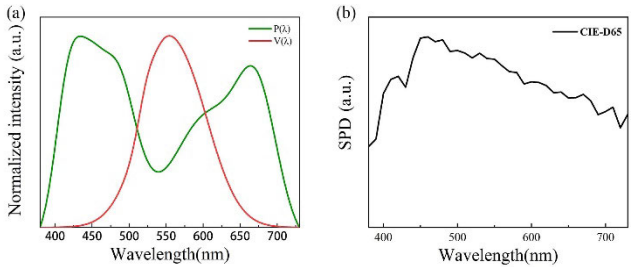

FIGURE 1. (a) The photopic sensitivity action curve V(λ) and the PAF curve P(λ), (b) the SPD of the CIE standard illuminant D65.

proposed to describe the SPD of a LED or other luminescent materials [28, 41]. Thereinto, double Gaussian model has been proved to be effective in simulating the narrow-band SPD of LED chips or QDs. By using of the double Gaussian model, the SPD of a single GaN chip or a single QD system is described as:

$$S_s(\lambda) = H_p \times \left[G(\lambda) + 2 \times G^5(\lambda)\right]/3 \tag{5}$$

where H_p is the peak height, $G(\lambda) = \exp\left[-\left(\lambda - \lambda_p\right)^2/\Delta\lambda^2\right]$, in which λ_p is the peak wavelength and $\Delta\lambda$ is the FWHM. For an artificial light source fabricated by integrating QDs of different emission bands with a purple or a blue GaN chip, its emission spectral is given as:

$$S(\lambda) = \sum_i S_{si}(\lambda) \tag{6}$$

where i represents the different color components.

III. SIMULATION RESULTS AND DISCUSSION

For the spectral simulation, a purple GaN chip with an emission wavelength 390 nm and an FWHM of 25 nm is used to integrate with QDs. Due to the size effect, the peak wavelengths λ_p of QDs can be tuned in a certain range. QDs of different systems demonstrate different emission ranges and FWHMs [42]–[44]. Here is this work, ternary II-VI and I-III-VI QDs are used to design the spectra of growing lamps.

A. SIMULATION RESULTS OF THREE-BAND QLEDs BASED ON CdZnS/ZnS AND CdZnS/ZnSe QDs

CdS and CdSe, and their core/shell structure QDs are investigated most extensively [45]. By alloying with Zn element and introducing ZnS or ZnSe shell, the photoluminescent quantum yields of CdZnS QDs can be enhanced remarkably[46]. Up to now, the emission wavelengths of CdZnS/ZnS and CdZnS/ZnSe have covered the whole visible range. Considering that $P(\lambda)$ has two high absorption peaks located at ~450 nm and ~660 nm respectively, the SPD of a three-band QLED based on a purple chip, blue emission CdZnS/ZnS QDs and red emission CdZnS/ZnSe QDs is calculated firstly by using of Equations (5) and (6). The peak wavelengths of the purple chip, the blue CdZnS/ZnS QDs and the red CdZnS/ZnSe QDs (denoted as λ_P, λ_B and λ_R respectively) are chosen to be 390 nm, 450 nm and 665 nm respectively, the corresponding emission FWHMs (denoted as $\Delta\lambda_P$, $\Delta\lambda_B$ and $\Delta\lambda_R$ respectively) are 20 nm, 10 nm and 55 nm respectively. Here, the corresponding peak heights of the purple chip, the blue and the red emission QDs (denoted as H_P, H_B and H_R respectively) are set firstly to be 10 mW/nm, 4 mW/nm and 9 mW/nm respectively. This three-band spectrum is shown as the black solid curve in Fig. 2(a). To characterize the photosynthesis performance of this device, both its photon quantities and photosynthetic quantities including PLER, LER, PAF and IPI are also calculated according to Equations (1)-(4). Its PLER, LER, PAF and IPI are calculated to be 404.785 plm/W, 50.047 lm/W, 8.088 and 4.012 respectively. Its figure-of-merits of visual performance such as CRI and color correlated temperature (CCT) are also calculated to be 47.776 and 1001 K respectively, as shown in Table 1.

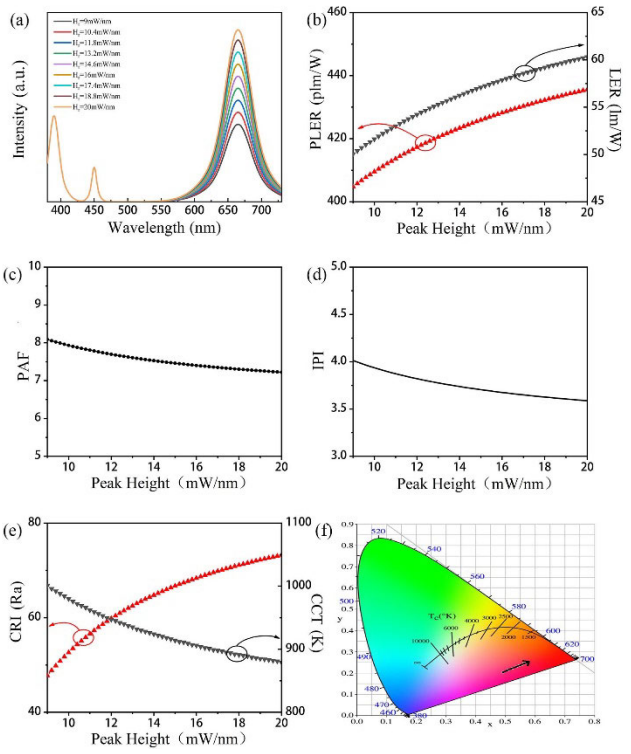

FIGURE 2. Optical, photosynthetic and visual properties of three-band QLEDs. (a) Spectrum, (b) PLER, (c) PAF, (d) IPI and (e) CRI and CCT varying with red emission height HR. (f) The evolution of color coordinates of the QLED with the increasing HR.

TABLE 1. Simulation results of three-band QLEDs.

H_R (mW/nm)	PLER (plm/W)	LER (lm/W)	PAF (plm/lm)	IPI	CRI	CCT (K)
9	404.785	50.047	8.088	4.012	47.776	1001
14	423.365	56.237	7.528	3.738	64.774	924
20	435.594	60.311	7.223	3.588	73.260	879

It can be calculated from Equation (3) that the IPI of a CIE stand illuminant, or the midday sun, is a unit. For

an artificial light source, its influence of photosynthesis to the plant is compared to that of the sun by using of the IPI. PAF means the percentage of the luminous flux driving photosynthesis accounting for that human eyes receive. The higher PAF is, the higher the luminous flux percentage used to drive photosynthesis. Conventional incandescent bulbs, metal halides and high pressure solidum lamps usually give PAFs smaller than 2 and IPIs smaller than one [17, 22]. It can be seen from Table 1 that this three-band QLED has both a much high PAF and a much high IPI than those of the incandescent bulbs, metal halides or high pressure solidum lamps. High match degree between the emission wavelengths of QDs and the high absorption peaks of P(λ) resulted from of QDs can be accounted for the high PAF and IPI values of this three-band QLED spectrum. Nevertheless, it shows a low CRI of 47.776 and a low CCT of 1001 K, which are uncomfortable for the visual experience of human eye. Spectrum components have influences both on the photosynthetic and the visual performances of the light source. By varying the FWHM of the blue or/and the red emission, or varying the spectrum height of the blue or/and the red emission, photosynthetic parameters including PLER, PAF and IPI, and visual ones including CRI and CCT can be adjusted. The emission height or luminous intensity will increase with the increase of driving voltage or driving current within a certain voltage or current range [47], [48]. Moreover, with a given voltage or current, the luminous intensity is also related to the QD concentration in the device [49]. Therefore, varying the peak height of the red CdZnS/ZnSe QDs is equivalent to examining the influence of the driving voltage or current of red QLED device or red QDs, or the concentration of red QDs on the spectral shape and so on. With the peak height of red emission H_R varying from 9 to 20 mW/nm, and the same other parameters as the black solid curve shown in Fig. 2a, spectrum curves, relative photosynthetic parameters and visual ones are calculated and shown in Fig. 2b-d respectively.

It can be seen from Fig. 2b that both PLER and LER increase with the increasing of H_R. On the contrary, both PAF and IPI show a decreasing trend with the increasing H_R. This declining is moderate. With $H_R = 20$ mW/nm, the PAF and the IPI are 8.088 and 4.012 respectively, which are still superior results in comparison with those of the incandescent bulbs etc. For visual performances, CRI increases, but CCT decreases with the increasing H_R. With H_R varying from 9 to 20 mW/nm, CRI increases from 47.776 to 73.260, and CCT decreases from 1001 to 879 K. CRI and CCT demonstrate these variation trends are ascribed to the addition of the red component, which is an important factor to obtain a light source with a high CRI and a warm color temperature. However, despite the high photosynthetic parameters of these three-band QLEDs, their CRI and CCT are not better than those reported white LEDs (WLEDs) [50], [51]. With the increasing of H_R, the color coordinates move into the deep-red region, as shown in Fig. 2f.

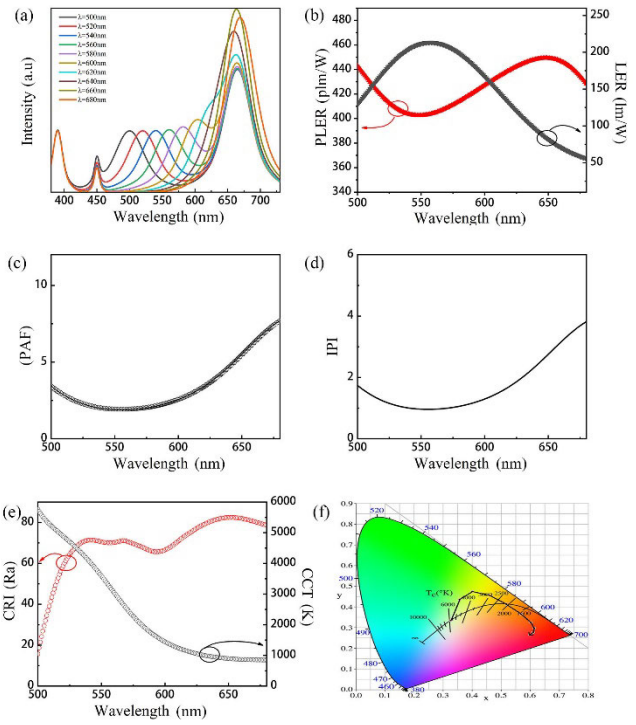

FIGURE 3. Optical, photosynthetic and visual properties of four-band QLEDs. (a) Spectrum, (b) PLER, (c) PAF, (d) IPI and (e) CRI and CCT varying with the fourth emission wavelength $\lambda 4$. (f) The evolution of color coordinates of the QLED with the increasing $\lambda 4$.

B. SIMULATION RESULTS OF FOUR-BAND QLEDs BASED ON CdZnS/ZnS AND CdZnS/ZnSe QDs

To enhance the visual performance, a fourth band emission between the blue and the red bands of the three-band SPD is considered. In the four-band simulation, we studied the influence of the newly added wavelength with fixed an emission height and an FWHM on the spectrum shape, and the photosynthetic and the visual performances as well.

With $H_R = 20$ mW/nm and other parameters the same with the curves in Figure 2a, the influence of peak emission wavelength of the fourth band on the photosynthetic and the visual performances of the QLEDs are investigated. With $H_4 = 4$ mW/nm (The footnote 4 denotes the fourth band), $\Delta\lambda_4 = 60$ nm and λ_4 varying from 500 to 680 nm, the spectra are calculated based on Equations (5) and (6) and shown in Fig. 3a. It can be seen from Fig. 3b that both the PLER and the LER of the four-band QLED exhibit a more variation trend than those of the three-band one. LER increases firstly, approaches a maximum value with $\lambda_4 = 550$ mm, which is the peak wavelength of the photopic spectral sensitivity function, and then decreases. However, LER varies in an opposite direction. As a result, PAF decreases firstly and then increases with λ_4 varying from 500 to 680 nm, and the minimum value is 1.89 with $\lambda_4 = 555$ nm. It is also calculated that IPI has almost the same variation trend with that of PAF, and it reaches its minimum value of 0.961 with $\lambda_4 = 554$ nm. For visual parameters, it can be seen from Fig. 3e

TABLE 2. Simulation results of four-band QLEDs.

λ (nm)	PLER (plm/W)	LER (lm/W)	PAF (plm/lm)	IPI	CRI	CCT (K)
520	417.688	171.622	2.434	1.235	58.854	4887
560	404.487	213.202	1.897	0.964	70.181	3051
600	427.193	166.945	2.559	1.296	66.542	1445
620	439.777	129.237	3.403	1.718	75.103	1110

that with λ_4 varying from 500 to 680 nm, CRI increases firstly and then decreases overall, and CCT shows a downward trend. With the increasing of λ_4, the color coordinates move into the red region finally along a tortuous path, as shown in Fig. 3f. Some of the simulation results are summarized in Table 2. Despite the photosynthetic performance of this four-band QLED shows no advantages, the visual parameters are somewhat superior in comparison to those of the three-band ones.

In short, there is a trade-off between the photosynthetic and the visual performances of a light source, and both the vision effects and the non-vision effects are related tightly with its spectrum shape and its color components. Our simulation results confirm that both peak wavelengths and peak heights have influences on the spectrum shape, so as to the photosynthetic and the visual performances. These preliminarily results may provide the designing and fabricating growing lamps with some instructions, and it is believed that a global optimization will outcome more effective results. Generally, by using of LEDs, white light can be achieved by using i) the arrangement and combination of multi-color LED chips and ii) the integration of a blue or a purple LED chip with the rare-earth phosphors [52, 53]. Nowadays, QD materials have also used as active materials to fabricate electroluminescent and photoluminescent LEDs. For electroluminescent QD-based LEDs (QLEDs), many devices of monochromatic light such as red, blue and green have been assembled [54]–[56]. As far as photoluminescent ones, both the devices with only QDs and those with the combination of QDs and rare-earth phosphors have also been fabricated [57]–[59]. Therefore, whether it is only using QDs as luminescent materials, or together with phosphors as luminescent materials, or monochromatic electroluminescent QLEDs together with LEDs as supplement, QD materials, whose luminous properties can be adjusted conveniently by changing the elementary composition, dot structures or synthesis conditions, will provide more flexible options for lighting design to meet different needs, including the growing lamps with satisfied photosynthetic and visual performances.

IV. EXPERIMENTAL RESULTS AND DISCUSSION

Previously, we synthesized ternary alloyed CdZnS QDs, and coated them with ZnS or ZnSe shell. The resulted CdZnS/ZnS

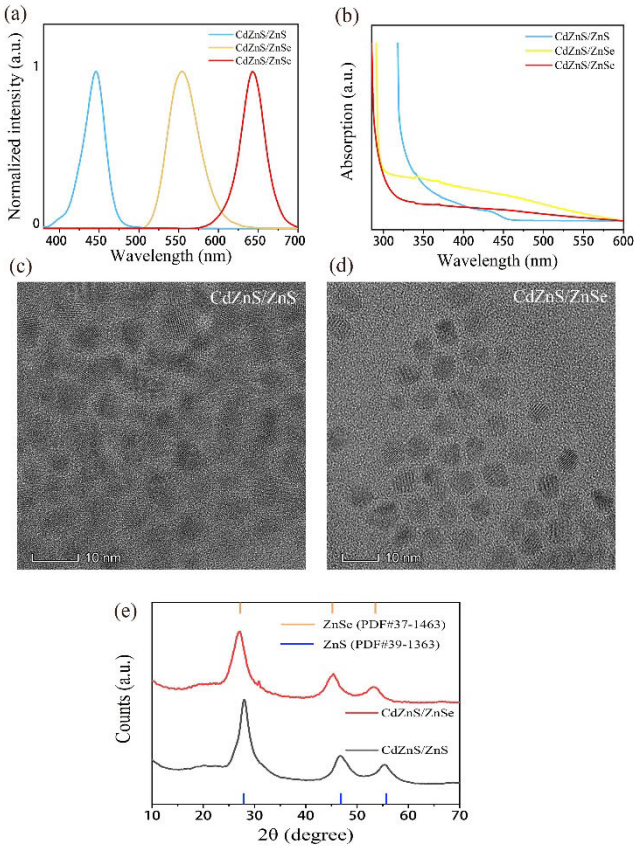

FIGURE 4. (a) PL, (b) UV-visible absorption spectra, of CdZnS/ZnS and CdZnS/ZnSe QDs. TEM images of (c) CdZnS/ZnS and (d) CdZnS/ZnSe QDs. (e) XRD patterns of CdZnS/ZnS and CdZnS/ZnSe QDs.

and CdZnS/ZnSe QDs emitted light covering nearly the whole visible wavelength range [29], [30]. Herein this work, by using of the same method, we synthesized blue emission CdZnS/ZnS (450 nm), green emission CdZnS/ZnSe (550 nm) and red emission CdZnS/ZnSe (650 nm) QDs. Their PL and the UV-visible absorption spectra shown in Figure 4a and 4b were recorded by using of a fluorescence spectrophotometer (F-97XP, LengGuang Tech.) and a spectrophotometer (UV-1800SPC, Macy Instrument) respectively. All these as synthesized QDs exhibit symmetrical PL spectra with narrow FWHMs of 30, 45 and 35 nm for the blue, green and red emission respectively. For the UV-vis absorption spectra shown in Figure 4b, the CdZnS/ZnS QDs show obvious the first exciton absorption peak at about 450 nm owning to their type-I QD structure. In contrast, no obvious the first exciton absorption peaks can be observed for the CdZnS/ZnSe QDs, because of the type-II structure resulted from their staggered energy levels. Transmission electron microscopy (TEM) images of CdZnS/ZnS and CdZnS/ZnSe QDs are shown in Figure 4c and 4d. Independent QD particles with spherical shape can be distinguished in these two images. X-ray diffraction (XRD) patterns of CdZnS/ZnS and CdZn/ZnSe QDs were also recorded to identify their crystal structures. It can be seen from Figure 4e that the characteristic peaks of CdZnS/ZnS locate at 27.962°, 46.83° and 55.459°

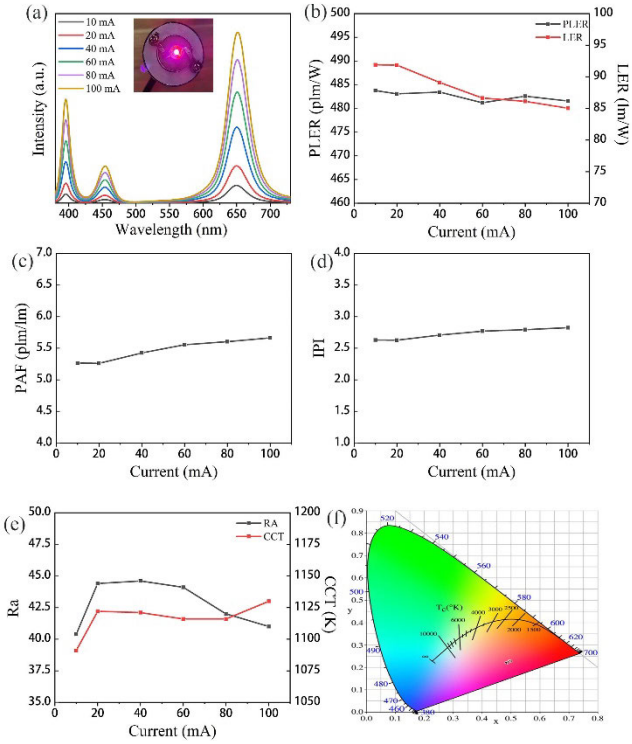

FIGURE 5. (a) Spectra, (b) PLER and LER, (c) PAF, (d) IPI, (e) Ra and CCT and (f) color coordinates of the three-band QLED under different driven currents. Inset in (a) is the digital photography of the device.

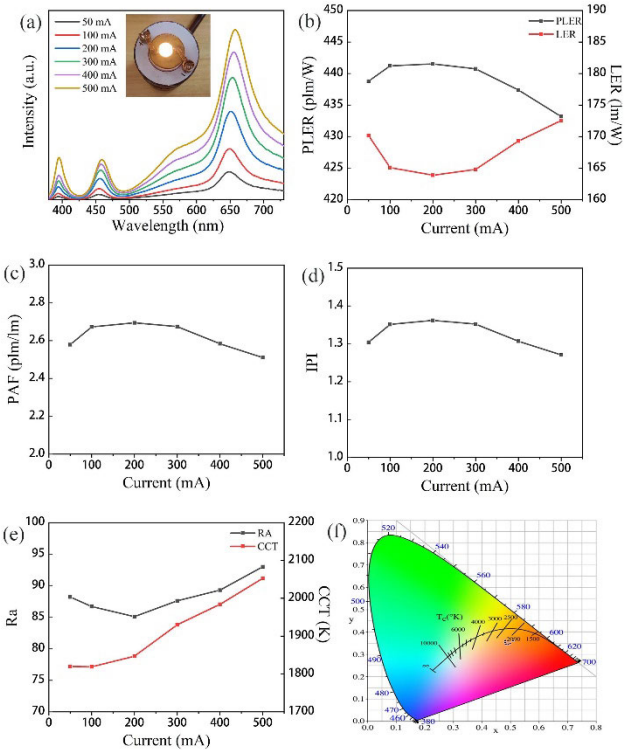

FIGURE 6. (a) Spectra, (b) PLER and LER, (c) PAF, (d) IPI, (e) Ra and CCT and (f) color coordinates of the four-band QLED under different driven currents.Inset in (a) is the digital photography of the device.

respectively, close to 27.857°, 46.865° and 55.695°, which are attributed to the wurtzite ZnS (JCPDS NO. 39-1363). For the QDs with ZnSe shell, their XRD characteristic peaks locate at 26.991°, 45.306° and 53.466°, close to 27.224°, 45.195° and 53.568°, which are attributed to the cubic ZnSe (JCPDS NO. 35-1469). This indicates that ZnS and ZnSe shell tend to coat the CdZnS cores.

The blue emission CdZnS/ZnS and red emission CdZnS/ZnSe QDs were employed to fabricate three-band QLEDs by exciting them with and LED chip peaked at 390 nm. The electroluminescence (EL) spectra of the device driven by different current are recorded by using an integrated test system (HP9000, HOPOO Optoelectronics Technology Co. Ltd.) and stacked in Figure 5a. The peak emission of the LED chip and the employed QDs all increased with driven current increasing from 10 to 100 mA with no obvious change in the spectrum shape. This device exhibits stable PLER values about 482.6 plm/W but decreasing LER values with the same current range, as shown in Figure 5b. It can be seen from Figure 5c and 5d that both the photosynthetic values of PAF and IPI increase with the ascending driven current. For the vision parameters, Ra increases firstly and then deceases, CCT shows an increasing trend overall. However, the highest Ra and CCT are 44.6 and 1130 K respectively, which are relatively low for human visual experience. As seen in Figure 5f, the color coordinates of the device locate in the red region with driven current varying from 10 to 100 mA.

To optimizing the vision performance of the QLED device, the 550-nm emission QDs were considered to fabricate the four-band QLEDs based on the three-band ones. The EL spectrum evolution with driven current varying from 50 to 500 mA is shown in Figure 6a. Different from the obvious emission peaks of the QDs for three-band device, the peak emission of the 550-nm emission is not easily to distinguish, especially under the relatively low applied current. Therefore, the emission intensity of this device increases with some spectrum shape change with the increasing driven current. For this four-band device, PLER increases firstly and then decreases, LER decreases firstly and then increases, resulted from the consistence of peak positions of the green-emission QDs and V(λ). PAF and IPI exhibit a same variation with increasing applied current, as shown in Figure 6c and 6d. the highest PLER, PAF and IPI of this four-band device are 441.5249 plm/W, 2.6942 and 1.3621, respectively, which are smaller than those of the three-band one. Nevertheless, this four-band QLED show higher PAF and IPI than those conventional light sources. Furthermore, it also exhibits higher CRI above 80 and improved CCT than those of the three-band one, as shown in Figure 6c. The highest Ra of the four-band device is 93, and the CCT values are in the range of 1819 – 2053 K. Obviously, the vision performance improves remarkably compared with those of the three-band one. With the integration of the 550-nm emission QDs, the color coordinates move from the red region to the yellow region, being helpful for improving the human visual experience.

V. CONCLUSION

Artificial lighting is essential for the off-season planting in indoor plant factories. Taking both the photosynthetic and the visual performances into account, spectrum of grow lamps based on QD materials are designed and optimized. Simulation results show that three-band QLEDs have much higher PAF and IPI than conventional light sources but poor visual performance such as low CRI. As far as the four-band QLED is concerned, its visual performance is enhanced with degenerate photosynthetic parameters. Despite this, calculation results show that the PAF and the IPI of the four-band QLEDs are still higher than those of the conventional light sources. In short, there is a trade-off between the photosynthetic and the visual performances, and this contradiction can be solved by use the light sources with high photosynthetic performances or high visual performances alternatively. CdZnS-based core/shell QDs with different emission wavelength are synthesized and employed as emitters to fabricate three-band and four-band QLEDs. The photosynthetic and the vision performances of the devices are also investigated and the obtained results show consistence with the simulation ones. This confirms the feasibility of fabricating growing lamps with QD materials. With more in-depth studies on the synthesis of QDs and the global optimization of the spectrum, low energy consumption and high efficiency QLEDs with satisfied photosynthetic performances and visual properties can be fabricated and applied to the field of growing lamps.

REFERENCES

[1] H. Murase, "Manufactureing vegetables in near future," *J. Jpn. Soc. Mech. Eng.*, vol. 116, no. 1132, pp. 116–117, 2013.
[2] J. Joshi, G. Zhang, S. Shen, K. Supaibulwatana, C. K. A. Watanabe, and W. Yamori, "A combination of downward lighting and supplemental upward lighting improves plant growth in a closed plant factory with artificial lighting," *Hortscience*, vol. 52, no. 6, pp. 831–835, Jun. 2017.
[3] Y. Hashimoto, "Computer integrated plant growth factory for agriculture and horticulture," *IFAC Proc. Volumes*, vol. 24, no. 11, pp. 105–110, Sep. 1991.
[4] S.-L. Zheng, L.-J. Wang, N.-X. Wan, L. Zhong, S.-M. Zhou, W. He, and J.-C. Yuan, "Response of potato tuber number and spatial distribution to plant density in different growing seasons in Southwest China," *Frontiers Plant Sci.*, vol. 7, p. 365, Apr. 2016.
[5] F. T. Tewolde, N. Lu, K. Shiina, T. Maruo, M. Takagaki, T. Kozai, and W. Yamori, "Nighttime supplemental LED inter-lighting improves growth and yield of single-truss tomatoes by enhancing photosynthesis in both winter and summer," *Frontiers Plant Sci.*, vol. 7, p. 448, Apr. 2016.
[6] K. Kitazaki, A. Fukushima, R. Nakabayashi, Y. Okazaki, M. Kobayashi, T. Mori, T. Nishizawa, S. Reyes-Chin-Wo, R. W. Michelmore, K. Saito, K. Shoji, and M. Kusano, "Metabolic reprogramming in leaf lettuce grown under different light quality and intensity conditions using narrow-band LEDs," *Sci. Rep.*, vol. 8, no. 1, Dec. 2018, Art. no. 7914.
[7] V.-D. Ngo, B.-E. Jang, S.-U. Park, S.-J. Kim, Y.-J. Kim, and S.-O. Chung, "Estimation of functional components of Chinese cabbage leaves grown in a plant factory using diffuse reflectance spectroscopy," *J. Sci. Food Agricult.*, vol. 99, no. 2, pp. 711–718, Jan. 2019.
[8] H. Watanabe, "Light-controlled plant cultivation system in Japan—Development of a vegetable factory using leds as a light source for plants," *Acta Hortic.*, vol. 907, pp. 37–44, 2011, doi: 10.17660/ActaHortic.2011.907.2.
[9] K. Li, Q.-C. Yang, Y.-X. Tong, and R. Cheng, "Using movable light-emitting diodes for electricity savings in a plant factory growing lettuce," *Horttechnology*, vol. 24, no. 5, pp. 546–553, Oct. 2014.
[10] C.-L. Chang, K.-P. Chang, and G.-B. Song, "Design and implementation of a cloud-based LED lighting control system for protected horticulture," *Appl. Eng. Agricult.*, vol. 32, no. 6, pp. 697–706, 2016.
[11] S. E. Balegh and O. Biddulph, "The photosynthetic action spectrum of the bean plant," *Plant Physiol.*, vol. 46, no. 1, pp. 1–5, Jul. 1970.
[12] J. B. Clark and G. R. Lister, "Photosynthetic action spectra of trees: I. Comparative photosynthetic action spectra of one deciduous and four coniferous tree species as related to photorespiration and pigment complements," *J. Plant Physiol.*, vol. 55, no. 2, pp. 401–406, 1975.
[13] F. T. Haxo and L. R. Blinks, "Photosynthetic action spectra of marine algae," *J. Gen. Physiol.*, vol. 33, no. 4, pp. 389–422, Mar. 1950.
[14] S. Cao, T. Han, Q. Li, L. Peng, C. Zhao, Y. Tang, and J. Xu, "Tunable spectrum resemblance of LED lights for improving the photosynthetic action of Chinese cabbages," *Life Sci. Space Res.*, vol. 26, pp. 28–33, Aug. 2020.
[15] L. Poulet, G. D. Massa, R. C. Morrow, C. M. Bourget, R. M. Wheeler, and C. A. Mitchell, "Significant reduction in energy for plant-growth lighting in space using targeted LED lighting and spectral manipulation," *Life Sci. Space Res.*, vol. 2, pp. 43–53, Jul. 2014.
[16] Z. Vokáčová and J. V. Burda, "Computational study on spectral properties of the selected pigments from various photosystems: Structure-transition energy relationship," *J. Phys. Chem. A*, vol. 111, no. 26, pp. 5864–5878, Jul. 2007.
[17] J. H. Oh, H. Kang, H. K. Park, and Y. R. Do, "Optimization of the theoretical photosynthesis performance and vision-friendly quality of multi-package purplish white LED lighting," *RSC Adv.*, vol. 5, no. 28, pp. 21745–21754, 2015.
[18] M. O. K. Azad, K. H. Kjaer, M. Adnan, M. T. Naznin, J. D. Lim, J. Sung, C. H. Park, and Y. S. Lim, "The evaluation of growth performance, photosynthetic capacity, and primary and secondary metabolite content of leaf lettuce grown under limited irradiation of blue and red LED light in an urban plant factory," *Agriculture*, vol. 10, no. 2, pp. 1–16, 2020.
[19] A. J. S. Neto, L. D. O. Moura, D. D. C. Lopes, L. D. A. Carlos, L. M. Martins, and L. D. C. L. Ferraz, "Non-destructive prediction of pigment content in lettuce based on visible-NIR spectroscopy," *J. Sci. Food Agricult.*, vol. 97, no. 7, pp. 2015–2022, May 2017.
[20] M. N. Kyewalyanga, T. Platt, and S. Sathyendranath, "Estimation of the photosynthetic action spectrum: Implication for primary production models," *Mar. Ecol. Prog.*, vol. 146, nos. 1–3, pp. 207–223, 1997.
[21] T. Wu, Y. Lin, L. Zheng, Z. Guo, J. Xu, S. Liang, Z. Liu, Y. Lu, T.-M. Shih, and Z. Chen, "Analyses of multi-color plant-growth light sources in achieving maximum photosynthesis efficiencies with enhanced color qualities," *Opt. Exp.*, vol. 26, no. 4, p. 4135, 2018.
[22] M. Aubé, J. Roby, and M. Kocifaj, "Evaluating potential spectral impacts of various artificial lights on melatonin suppression, photosynthesis, and star visibility," *PLoS ONE*, vol. 8, no. 7, Jul. 2013, Art. no. e67798.
[23] *Optical Radiation Physics and Illuminating Engineering—Part 10: Photobiologically Effective Radiation, Quantities, Symbols and Action Spectra*, German National Standard DIN 5031-10, Deutshes Institut Fur NormungEV, Berlin, Germany, 2000.
[24] V. Awate, R. Tiwari, A. K. Shrivastava, N. Dubey, and V. Dubey, "Synthesis, characterization and luminescence studies of rare Earth activated Sr_2SiO_4 phosphor: A review," *J. Mater. Sci., Mater. Electron.*, vol. 29, no. 6, pp. 4391–4401, Mar. 2018.
[25] X. Peng, "An essay on synthetic chemistry of colloidal nanocrystals," *Nano Res.*, vol. 2, no. 6, pp. 425–447, Jun. 2009.
[26] M. A. Boles, D. Ling, T. Hyeon, and D. V. Talapin, "The surface science of nanocrystals," *Nature Mater.*, vol. 15, no. 3, p. 364, 2016.
[27] Y.-L. Lee and Y.-S. Lo, "Highly efficient quantum-dot-sensitized solar cell based on co-sensitization of CdS/CdSe," *Adv. Funct. Mater.*, vol. 19, no. 4, pp. 604–609, Feb. 2009.
[28] Z.-Q. Guo, T.-M. Shih, Y.-J. Lu, Y.-L. Gao, L.-H. Zhu, G.-L. Chen, J.-H. Zhang, S.-Q. Lin, and Z. Chen, "Studies of scotopic/photopic ratios for color-tunable white light-emitting diodes," *IEEE Photon. J.*, vol. 5, no. 4, Aug. 2013, Art. no. 8200409.
[29] F. Li, L. You, C. Nie, Q. Zhang, X. Jin, H. Li, X. Gu, Y. Huang, and Q. Li, "Quantum dot white light emitting diodes with high scotopic/photopic ratios," *Opt. Exp.*, vol. 25, no. 18, pp. 21901–21913, 2017.
[30] F. Li, L. You, H. Li, X. Gu, J. Wei, X. Jin, C. Nie, Q. Zhang, and Q. Li, "Emission tunable CdZnS/ZnSe core/shell quantum dots for white light emitting diodes," *J. Lumin.*, vol. 192, pp. 867–874, Dec. 2017.
[31] M. Yang, Y. Wang, Y. Ren, E. Liu, J. Fan, and X. Hu, "Zn/Cd ratio-dependent synthetic conditions in ternary ZnCdS quantum dots," *J. Alloys Compounds*, vol. 752, pp. 260–266, Jul. 2018.

[32] Z. Li, F. Chen, L. Wang, H. Shen, L. Guo, Y. Kuang, H. Wang, N. Li, and L. S. Li, "Synthesis and evaluation of ideal core/shell quantum dots with precisely controlled shell growth: Nonblinking, single photoluminescence decay channel, and suppressed FRET," *Chem. Mater.*, vol. 30, no. 11, pp. 3668–3676, Jun. 2018.

[33] P. Reiss, M. Protière, and L. Li, "Core/shell semiconductor nanocrystals," *Small*, vol. 5, no. 2, pp. 154–168, Jan. 2009.

[34] Y. Jang, A. Shapiro, M. Isarov, A. Rubin-Brusilovski, A. Safran, A. K. Budniak, F. Horani, J. Dehnel, A. Sashchiuk, and E. Lifshitz, "Interface control of electronic and optical properties in IV–VI and II–VI core/shell colloidal quantum dots: A review," *Chem. Commun.*, vol. 53, no. 6, pp. 1002–1024, 2017.

[35] P. A. Mykland and L. Zhang, "The double Gaussian approximation for high frequency data," *Scand. J. Statist.*, vol. 38, no. 2, pp. 215–236, Jun. 2011.

[36] M. G. Figueiro, "Disruption of circadian rhythms by light during day and night," *Current Sleep Med. Rep.*, vol. 3, no. 2, pp. 76–84, Jun. 2017.

[37] Z. Ma, S. Li, M. Zhang, S. Jiang, and Y. Xiao, "Light intensity affects growth, photosynthetic capability, and total flavonoid accumulation of anoectochilus plants," *Hortscience*, vol. 45, no. 6, pp. 863–867, Jun. 2010.

[38] K. R. Cope, M. C. Snowden, and B. Bugbee, "Photobiological interactions of blue light and photosynthetic photon flux: Effects of monochromatic and broad-spectrum light sources," *Photochem. Photobiol.*, vol. 90, no. 3, p. 574, 2014.

[39] S. Takita, K. Okamoto, and T. Yanagi, "Computer simulation of PPF distribution under blue and red LED light source for plant growth," *Acta Horticulturae*, vol. 440, no. 440, pp. 286–291, 1997.

[40] R. A. McKinnon and F. J. J. Clarke, "Problem of simulating daylight for the illumination of fluorescent materials," *Proc. SPIE*, vol. 262, pp. 87–93, Feb. 1982.

[41] G. Ziquan, T. Shih, Y. Gao, Y. Lu, L. Zhu, G. Chen, Y. Lin, J. Zhang, and Z. Chen, "Optimization studies of two-phosphor-coated white light-emitting diodes," *IEEE Photon. J.*, vol. 5, no. 2, Apr. 2013, Art. no. 8200112.

[42] X. Kang, L. Huang, Y. Yang, and D. Pan, "Scaling up the aqueous synthesis of visible light emitting multinary $AgInS_2$/ZnS core/shell quantum dots," *J. Phys. Chem. C*, vol. 119, no. 14, pp. 7933–7940, Apr. 2015.

[43] A. A. Rossinelli, A. Riedinger, P. Marqués-Gallego, P. N. Knüsel, F. V. Antolinez, and D. J. Norris, "High-temperature growth of thick-shell CdSe/CdS core/shell nanoplatelets," *Chem. Commun.*, vol. 53, no. 71, pp. 9938–9941, 2017.

[44] K.-H. Lee, J.-H. Lee, H.-D. Kang, C.-Y. Han, S. M. Bae, Y. Lee, J. Y. Hwang, and H. Yang, "Highly fluorescence-stable blue CdZnS/ZnS quantum dots against degradable environmental conditions," *J. Alloys Compounds*, vol. 610, pp. 511–516, Oct. 2014.

[45] S. Bisschop, P. Geiregat, T. Aubert, and Z. Hens, "The impact of core/shell sizes on the optical gain characteristics of CdSe/CdS quantum dots," *ACS Nano*, vol. 12, no. 9, pp. 9011–9021, Sep. 2018.

[46] H. Shen, C. Zhou, S. Xu, C. Yu, H. Wang, X. Chen, and L. S. Li, "Phosphine-free synthesis of $Zn_{1-x}Cd_xSe$/ZnSe/$ZnSe_xS_{1-x}$/ZnS core/multishell structures with bright and stable blue–green photoluminescence," *J. Mater. Chem.*, vol. 21, no. 16, p. 6046, 2011.

[47] C. Guo, Y. Huang, Q. Pan, T. Tao, F. Li, Q. Zhang, X. Jin, and Q. Li, "The role of deep-red emission $CuInS_2$/ZnS QDs in white light emitting diodes," *Semicond. Sci. Technol.*, vol. 34, no. 3, Mar. 2019, Art. no. 035025.

[48] C. Y. Kong, C.-H. Lin, C.-H. Lin, T.-Y. Li, S.-W. H. Chen, C.-L. Tsai, C.-W. Sher, T.-Z. Wu, P.-T. Lee, X. Xu, M. Zhang, C.-H. Ho, J.-H. He, and H.-C. Kuo, "Highly efficient and stable white light-emitting diodes using perovskite quantum dot paper," *Adv. Sci.*, vol. 6, no. 24, 2019, Art. no. 1902230.

[49] T. Zhang, H. Zhao, D. Riabinina, M. Chaker, and D. Ma, "Concentration-dependent photoinduced photoluminescence enhancement in colloidal PbS quantum dot solution," *J. Phys. Chem. C*, vol. 114, no. 22, pp. 10153–10159, Jun. 2010.

[50] J. H. Oh, S. J. Yang, and Y. R. Do, "Healthy, natural, efficient and tunable lighting: Four-package white LEDs for optimizing the circadian effect, color quality and vision performance," *Light, Sci. Appl.*, vol. 3, no. 2, p e141, Feb. 2014.

[51] H. S. Jang, H. Yang, S. W. Kim, J. Y. Han, S.-G. Lee, and D. Y. Jeon, "White light-emitting diodes with excellent color rendering based on organically capped CdSe quantum dots and Sr_3SiO_5: $Ce^{(3+)}$, $Li^{(+)}$ phosphors," *Adv. Mater.*, vol. 20, no. 14, pp. 2696–2702, 2008.

[52] S. Muthu, F. J. P. Schuurmans, and M. D. Pashley, "Red, green, and blue LEDs for white light illumination," *IEEE J. Sel. Topics Quantum Electron.*, vol. 8, no. 2, pp. 333–338, Mar./Apr. 2002.

[53] L. T. T. Vien, N. Tu, D. X. Viet, D. D. Anh, D. H. Nguyen, and P. T. Huy, "Mn^{2+}-doped Zn_2SnO_4 green phosphor for WLED applications," *J. Lumin.*, vol. 227, Nov. 2020, Art. no. 117522.

[54] Y. Yang, Y. Zheng, W. Cao, A. Titov, J. Hyvonen, J. R. Manders, J. Xue, P. H. Holloway, and L. Qian, "High-efficiency light-emitting devices based on quantum dots with tailored nanostructures," *Nature Photon.*, vol. 9, no. 4, pp. 259–266, Apr. 2015.

[55] B. S. Mashford, M. Stevenson, Z. Popovic, C. Hamilton, Z. Zhou, C. Breen, J. Steckel, V. Bulovic, M. Bawendi, S. Coe-Sullivan, and P. T. Kazlas, "High-efficiency quantum-dot light-emitting devices with enhanced charge injection," *Nature Photon.*, vol. 7, no. 5, pp. 407–412, May 2013.

[56] H. Shen, W. Cao, N. T. Shewmon, C. Yang, L. S. Li, and J. Xue, "High-efficiency, low turn-on voltage blue-violet quantum-dot-based light-emitting diodes," *Nano Lett.*, vol. 15, no. 2, pp. 1211–1216, Feb. 2015.

[57] D. Chen, G. Fang, and X. Chen, "Silica-coated Mn-doped $CsPb(Cl/Br)_3$ inorganic perovskite quantum dots: Exciton-to-Mn energy transfer and blue-excitable solid-state lighting," *ACS Appl. Mater. Interfaces*, vol. 9, no. 46, pp. 40477–40487, Nov. 2017, doi: 10.1021/acsami.7b14471.

[58] X. Hu, Y. Xie, C. Geng, S. Xu, and W. Bi, "Study on the color compensation effect of composite orange-red quantum dots in WLED application," *Nanosc. Res. Lett.*, vol. 15, no. 1, p. 118, Dec. 2020.

[59] R. F. Wang, J. L. Zhang, X. M. Xu, Y. L. Wang, L. Y. Zhou, and B. Li, "White LED with high color rendering index based on $Ca_8Mg(SiO_4)_{(4)}Cl^{-2}$: Eu^{2+} and ZnCdTe/CdSe quantum dot hybrid phosphor," *Mater. Lett.*, vol. 84, pp. 24–26, Oct. 2012.

ZILEI LIU was born in Taian, Shandong, China, in 1996. He received the B.S. degree in photoelectric science information and engineering from Binzhou University, in 2018. He is currently pursuing the master's degree in optical engineering with Nanchang Hangkong University. Since 2018, he has been a graduate student of the Jiangxi Engineering Laboratory for Optoelectronics Testing Technology, Nanchang Hangkong University. His research interests are quantum dot luminescent materials, including the synthesis of quantum dots and their application as light sources in plant lighting.

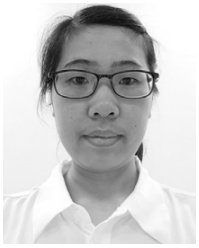

FENG LI was born in Honghu, Hubei, China, in 1981. She received the B.S. degree in physics from Hubei Normal University, in 2002, the M.S. degree in theoretical physics from Southwest China Normal University, in 2005, and the Ph.D. degree in measuring and test techniques and instrument from the College of Automation Engineering, Nanjing University of Aeronautics and Astronautics, in 2014. Since 2005, she has been a Teacher with the School of Measuring and Optical Engineering, Nanchang Hangkong University. She is the author of more than 40 articles. Her research interests include quantum dot materials and applications, light-emitting diodes and applications, and micro-nano structures and applications.

GAOXIANG HUANG was born in Gaoan, Jiangxi, China, in 1994. He received the B.S. degree in software engineering from the Jiangxi University of Technology, in 2018. He is currently pursuing the master's degree in optical engineering with Nanchang Hangkong University. Since 2018, he has been a postgraduate student of technology with the Nanchang Hangkong University. His research interests include the synthesis of environment friendly quantum dot materials and their applications in light-emitting diodes for health lighting.

JIAHU WEI was born in Yongzhou, Hunan, China, in 1994. He received the bachelor's degree in electronic information science and technology from Yibin University, in 2017, and the master's degree in optical engineering from Nanchang Hangkong University, in 2020. His research interest lies in environmentally friendly quantum dot luminescent materials, including the synthesis of quantum dots and their applications in light-emitting diodes and solar cells.

GUANGYU JIANG was born in Jingzhou, Hubei, China, in 1979. He received the M.S. degree in optics from Southwest University, Chongqing, China, in 2006, and the Ph.D. degree in optical engineering from the Nanjing University of Aeronautics and Astronautics, Nanjing, China, in 2016, respectively. He is currently a Lecturer with the School of Measuring and Optical Engineering, Nanchang Hangkong University, Nanchang, China. He has authored/coauthored more than 40 journal publications. His current research interests include in the nonlinear dynamics of semiconductor lasers and their applications, optical fiber communication, fiber sensor, optical design, and laser detection technology.

YAN HUANG received the M.S. degree in condensed matter physics from the Southwest China Normal University, in 2005, and the Ph.D. degree in mechanical design and theory from Beijing Jiaotong University, in 2015. His research interests include the synthesis of quantum dots and their application to luminescent devices.

XIAO JIN received his training in physics from the Harbin Institute of Technology (graduated in 2006) and received the Ph.D. degree in optics from the Harbin Institute of Technology, in 2011. Subsequently, he worked at Nanchang Hangkong University. He is currently an Associate Professor at Lingnan Normal University. His research interests include the synthesis of quantum dots and their application to optoelectronic devices.

QINGHUA LI received the M.S. degree from Huaqiao University, in 2007, and the Ph.D. degree in materials science from Huaqiao University. Subsequently, he worked at Nanchang Hangkong University. He is currently a Professor at Lingnan Normal University. His research interests include the synthesis of quantum dots and their application to optoelectronic devices.